

Clare Knock,<sup>1</sup> Ph.D. and Marie Davison,<sup>1</sup> M.Sc.

## Predicting the Position of the Source of Blood Stains for Angled Impacts

**ABSTRACT:** Droplets of pig's blood were dropped onto paper at different angles to the horizontal to produce blood stains. Impact velocities varied from 1.82 to 5.76 m/sec, drop size from 3.7 to 5.0 mm in diameter, and the surface sloped at angles between 22.7° and 90° to the horizontal. From the data a single equation relating stain size to drop size and velocity for all impact angles was produced;  $ab = 111.74 (\text{Re}^{1/2} \text{We}^{1/4})^{0.75} D_o D_o + 0.00084$  with  $R^2 = 0.88$ , where  $a$  is the stain width,  $b$  the stain length,  $\text{Re}$  the Reynolds number, and  $\text{We}$  the Weber number. A second equation related the number of spines,  $N$ , to drop size, velocity, and surface slope for all impact angles as  $N = 0.76 \text{We}^{0.5} \sin^3 \theta$  with  $R^2 = 0.9$ , where  $\theta$  is the impact angle. Combining these equations the impact velocity can be determined and hence the position of the stain's source.

**KEYWORDS:** forensic science, bloodstain pattern analysis, angled impact, spines, pig's blood

The standard technique for determining the position of the source of a blood stain at a crime scene is the "stringing technique" (1,2). This technique uses the fact that the width to length ratio of a blood stain is approximately related to its impact angle. Using the calculated angle of impact, a straight line is drawn back from the stain along the line of the impact angle. Where the lines from several stains intersect is assumed to be the source of the stain.

However, this does not take into account the effect of gravity on the flight path of the blood droplet. Assuming that the path of the blood stain can be described by the equations for the movement of a rigid object, i.e., neglecting factors such as air resistance and oscillation of the blood droplet, then the equations needed to include gravity in the flight path of the blood droplet are (3):

$$u_i \cos \theta_i = u_f \cos \theta_f \quad (1)$$

$$u_i \sin \theta_i - gt = u_f \sin \theta_f \quad (2)$$

$$x_f = x_o + u_i \cos \theta_i t \quad (3)$$

$$y_f = y_o + u_i \sin \theta_i t - \frac{1}{2}gt^2 \quad (4)$$

where  $(x_o, y_o)$ , are the coordinates of the source of the blood drop;  $(x_f, y_f)$  the position of the centre of the blood stain;  $\theta_i$ , the angle to the horizontal at which the drop is launched;  $\theta_f$ , the angle to the horizontal at which the drop hits the ground (or wall);  $u_i$ , the initial velocity of the droplet;  $u_f$ , the impact velocity of the droplet;  $t$ , time; and  $g$ , gravity. Eliminating the initial angle of flight, the initial velocity, and time gives:

$$y_o = y_f - \tan \theta_f (x_f - x_o) - \frac{0.5g(x_f - x_o)^2}{u_f^2 \cos^2 \theta_f} \quad (5)$$

Now the final position of the stain is known, the horizontal position of the source can be obtained by the stringing method

<sup>1</sup>Engineering Systems Department, Cranfield University, Shrivenham, Swindon, Wilts SN6 8BB, U.K.

Received 20 May 2006; and in revised form 2 Jan. 2007, 2 Mar. 2007; accepted 18 Mar. 2007; published 23 July 2007.

and this leaves two unknowns, the vertical position of the source and the impact velocity when the drop hits the wall or floor. If the latter can be determined from the stain shape and size then the position of the source of the blood can be obtained.

A large amount of work has been carried out looking at the vertical impact of droplets onto different (dry) surfaces to study the reverse problem, given a known drop size and impact velocity what will the final shape of the liquid stain be for the cases when no splashing occurs; for ink used in printing (4) and for water (5,6) because of its use in irrigation (7,8) and settling dust on coal (9).

The authors found that the stain's maximum size (10), final size (11) [as droplets hit a surface they expand out due to momentum and then contract back due to surface tension giving a final stain size smaller than the maximum spread of the impacting droplet (8)], number of spines (also termed fingers) (6,11), and any rebound of the droplet (12) depended on the droplet's impact velocity and size as well as a combination of surface tension, density, viscosity, and contact area (11).

When studying blood stains at a crime scene the maximum stain size or any rebound cannot be determined. This leaves the stain's size and number of spines from which to determine the impact velocity. A variety of equations relating the stain's size and number of spines have been determined. Some are physics based, looking at the stain size; the conservation of volume (4) or energy (8) or the forces acting on the drop (9) or to predict the number of spines; the Rayleigh–Taylor instability (5), or surface tension (13). Other equations require complex computer modeling (7,14,15). A survey of the papers prior to 1993 is given in Ref. (11) and later work on the number of spines occurring is summarized in Ref. (5).

In general, the equations developed in the above references were found not to work when the authors of this paper applied them to blood or water droplets. This may be due to the background of the work. Many projects were set up to examine the spraying of liquids onto surfaces (5) for use in spray painting or pesticide application, resulting in low Reynolds and Weber numbers (16).

In 2005, Hulse-Smith et al. (17) showed that it is possible to determine the impact velocity of a blood droplet landing vertically from the number of spines around the blood stain and the stains

size. By dropping different sized blood droplets onto a variety of surfaces from different heights they obtained the following equations.

$$\frac{D_s}{D_o} = C_d \frac{Re^{0.25}}{2} \tag{6}$$

and

$$N = C_N \sqrt{We} \tag{7}$$

where  $D_s$  is the final stain diameter,  $D_o$  the drop diameter,  $N$  the number of spines, and  $Re$  the Reynolds number defined by:

$$Re = \frac{\rho D_o V_o}{\mu} \tag{8}$$

where  $\mu$  is the viscosity,  $\rho$  the density, and  $V_o$  the impact velocity. The Weber number,  $We$ , is given by:

$$We = \frac{\rho D_o V_o^2}{\sigma} \tag{9}$$

where  $\sigma$  is the surface tension.  $C_N$  and  $C_d$  are constants, using experimental data (17) obtains values of 0.955 and 1.11, respectively, whilst working with water droplets authors obtained values of  $C_N = 1.14$  (5) and  $C_d = 1.0$  (18).

A theoretical parameter,  $Re_I$  proportional to the Weber and Reynolds number, defined as

$$Re_I \propto Re^{1/2} We^{1/4} \tag{10}$$

has been used (16). The authors found correlations for experimental data for a variety of liquids against Reynolds numbers of up to 25,000 and Weber numbers of up to 4000 for  $Re_I$  against the number of spines and the ratio of stain size to drop size. This paper is referenced in Ref. (5) but with the equation now (mis)printed as

$$Re_I \propto (Re^{1/2} We^{1/4})^{0.75} \tag{11}$$

hereafter referred to as  $Re_{IM}$ .

However, the above work only considered the vertical impact of blood stains and many blood stains arrive at an angle to the surface. Whilst there has been a large amount of work considering the vertical impact of droplets as outlined above, there has been little work on the angled impact of droplets, the exceptions were either onto a heated surface (19) or a single case at a single angle of 45° to validate a complex computational fluid dynamics model of the flow of a droplet but ignoring the generation of spines (20).

By looking at the angled impacts of blood droplets onto paper this paper shows how the same equations can be used to determine the impact velocity of droplets over a wide range of angles, for which the vertical impact is simply a special case.

**Experimental Technique**

As in the work in Ref. (17), pig’s blood was used, which has been shown to be a viable blood substitute (21). One liter of blood was mixed with 100 mL of the anticoagulant 10% sodium citrate. Blood was collected from the abattoir one morning and the blood to be used that day was kept in a water bath at 37°C and removed only when it was to be used, ensuring that the experiments were carried out at body temperature. The remaining blood was kept in a fridge to be used the following day. All blood was discarded at the end of the second day. Values for the density (1062 kg/m<sup>2</sup>),

viscosity (0.0048 N sec/m<sup>2</sup>), and surface tension (0.0056 N/m<sup>1</sup>) for pig’s blood were taken from the literature (21).

The blood was dropped from pipettes clamped into position at heights of 50, 100, 150, and 200 cm above the impact surface, resulting in impact velocities of 1.8–5.8 m/sec. Three different pipette sizes were used, 1.52, 2.25, and 5 mm diameter, to obtain different sized droplets, resulting in measured drop diameters of 3.4–5.0 mm. The pipette was changed every six drops to avoid clotting of blood affecting the drop size formed. The droplet fell vertically to impact onto a surface, the slope of which was altered to give impact angles of 22.7, 43.5, 56.3, 61.6, 78.8, and 90° to the horizontal. For the 22.7° impact only the 1.52 mm pipette was used and for the small pipette at 90° to the horizontal, extra heights of 20, 40, 60, and 80 cm were included. The surface used was standard photocopying paper. Each combination of height, pipette size, and surface slope was repeated six times.

The last 10 cm of the droplets fall was recorded using a Phantom V7.1 camera (Vision Research Inc., Wayne, NJ) filming at 1000 frames/sec. The drop’s velocity and width were measured using the camera’s image processing software, Phantom 7, camera software version 605.2. Whilst the droplets were formed slowly using the pipette to avoid imparting an initial velocity onto the droplet, measuring the drop’s velocity using the camera meant that if inadvertently an initial velocity was imparted onto the droplet, it was taken into account in the results. For all stains the stain size was measured and the number of spines around the entire stain (360°) was counted by hand. For each angle and height, the results were averaged over the six replicates. The stain size and number of spines were then plotted against a number of variables to obtain a correlation coefficient.

**Results**

Figure 1 shows the effect of impact angle on the number of spines obtained and the stain size and shape. As shown in previous work (1), as the impact angle increases, i.e., becomes closer to a vertical impact, the stain becomes shorter, until for a vertical impact a circular stain is generated (Fig. 1a). What has not been discussed before is that the number of spines also alters as the impact angle alters. From Fig. 1, it can be seen that the number of spines increases as the impact angle increases. As the drop size or impact velocity increase the stain size and number of spines also increases for an angled impact, Figs. 2 and 3, respectively, as previously demonstrated in Ref. (17) for a vertical impact.

**Vertical Impact**

To compare the results against work by previous authors, at first only vertical impacts were considered with the correlation coefficients,  $R^2$ , given in Table 1 for stain size and Table 2 for number

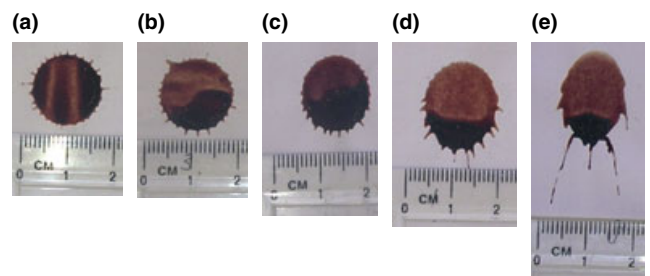


FIG. 1—Blood stains falling from 100 cm for a medium sized pipette at angles of (a) 90°, (b) 78.8°, (c) 61.6°, (d) 43.5°, and (e) 33.7° to the vertical.

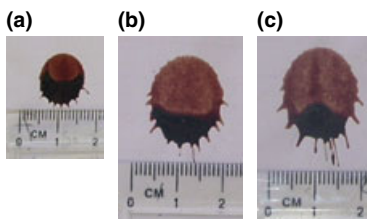


FIG. 2—Blood stains falling from 100 cm onto paper at an angle of 56.3° for drop sizes of (a) 3.83, (b) 4.4, and (c) 4.7 mm.

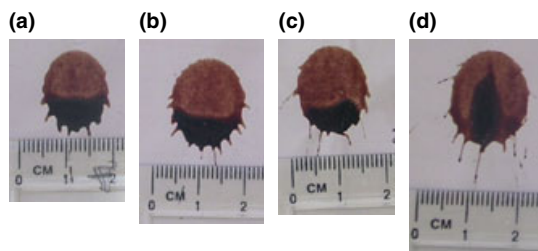


FIG. 3—Blood stains falling onto paper at an angle of 56.3° from heights of (a) 50, (b) 100, (c) 150, and (d) 200 cm.

of spines plotted against a number of parameters. When the stain size is plotted against the Reynolds number or Weber number the correlation is low as would be expected when plotting a dimensional number against a nondimensional number.

The circular stain produced by a vertical impact can be parameterized by the stain's diameter,  $D_s$ . To nondimensionalize the stain size for vertical impact, most work uses the ratio of the stain diameter to the drop size,  $D_s/D_o$  (17). This ratio is often known as  $\beta$  (11). However, on a sloping surface the stain is oval in shape (see for example Fig. 1c) and so the stain size,  $S$ , depends on both the stain's width ( $a$ ) and length ( $b$ ), and is given by  $S = \pi ab/4$ . So for the two-dimensional analysis, a new parameter has been developed during this work,  $\alpha$ , given by:

$$\alpha = \frac{ab}{D_o^2} \tag{12}$$

In the case of a vertical impact when a spherical stain is produced and therefore  $a = b$  this reduces to the form:

$$\alpha = \frac{ab}{D_o^2} = \frac{a^2}{D_o^2} = \beta^2 \tag{13}$$

Hence to plot results equivalent to those in Ref. (17), here given in Eq. (6), of beta against  $Re^{0.25}$  means squaring both sides of the equation and gives an equation of the form:

$$\alpha = mRe^{0.5} + c \tag{14}$$

or on expansion

$$ab = m \left( \frac{\rho u D_o}{\mu} \right)^{0.5} D_o^2 + c D_o^2 \tag{15}$$

where  $m$  and  $c$  are constants obtained from fitting a straight line to the data and  $c = 0$  in Eq. (6) from Ref. (17).

Plotting alpha against the Weber number gives a low correlation coefficient, but against the Reynolds number,  $Re_t$  and  $Re_{IM}$ , significant correlations were obtained (Table 1). For  $Re^{0.5}$  the equation is:

TABLE 2—Correlation coefficients,  $R^2$  for the number of spines against various parameters and where this is significant, the fitted equation for the experimental results.

Equation fitted	Vertical impact, 90°		All data	
	$y = mx + c$	$y = mx$	$y = mx + c$	$y = mx$
$N$ vs. $Re$	0.87 $y = 0.0060x + 4.26$	0.84 $y = 0.007x$	0.29	0.29
$N$ vs. $We$	0.76	0.10	0.21	0.07
$N$ vs. $We^{0.5}$	0.82 $y = 0.617x + 4.16$	0.80 $y = 0.72x$	0.21	0.21
$N$ vs. $Re_t$	0.85 $y = 0.61x + 4.11$	0.82 $y = 0.071x$	0.26	0.26
$N$ vs. $RE_{IM}$	0.86 $y = 0.35x - 2.82$	0.85 $y = 0.321x$	0.25	0.24

For an explanation of the symbols see text.

TABLE 1—Correlation coefficients,  $R^2$  for stain size against various parameters and where this is significant, the fitted equation for the experimental results.

Equation fitted	Vertical impact, 90°		All data	
	$y = mx + c$	$y = mx$	$y = mx + c$	$y = mx$
$S$ vs. $Re$	0.67	0.66	0.57	0.57
$S$ vs. $We$	0.52	0.021	—	—
$S$ vs. $ReD_oD_o$	0.92	0.89	0.86	0.80
$S$ vs. $Re_tD_oD_o$	$y = 0.2096 + 0.0026$	$y = 0.244x$	$y = 0.208 + 0.0042$	$y = 0.261x$
$S$ vs. $RE_{IM} D_oD_o$	0.9	0.89	0.85	0.81
$S$ vs. $RE_{IM} D_oD_o$	$y = 2.19x + 0.00223$	$y = 2.5x$	0.88	0.88
$\alpha$ vs. $Re$	0.95	0.94	0.88	0.88
$\alpha$ vs. $Re^{0.5}$	$y = 11.95x - 0.00091$	$y = 11.37x$	$y = 11.74x + 0.00084$	$y = 12.25x$
$\alpha$ vs. $We$	0.90	0.81	0.79	0.70
$\alpha$ vs. $Re_t$	$y = 0.0024x + 3.02$	$y = 0.0031x$	$y = 0.0023x + 3.27$	$y = 0.00312x$
$\alpha$ vs. $RE_{IM}$	0.91	0.83	0.80	0.48
$\alpha$ vs. $We$	$y = 0.183x - 5.22$	$y = 0.201x$	$y = 0.283x - 5.22$	$y = 0.201x$
$\alpha$ vs. $Re_t$	0.80	0.51	0.67	0.60
$\alpha$ vs. $RE_{IM}$	0.88	0.79	0.68	0.53
$\alpha$ vs. $RE_{IM}$	$y = 1.91x + 232.5$	0.89	0.68	0.69
	$y = 10.99x + 20.0$	$y = 11.21x$		

$$ab = 0.183 \left( \frac{\rho u D_o}{\mu} \right)^{0.5} D_o^2 - 5.22 D_o^2 \quad (16)$$

For this equation, as the velocity tends to zero the stain size tends to a negative area. Physically the impact velocity is zero when a drop is placed on the surface and allowed to collapse under gravity to produce a stain of finite size. Hence *c* in Eq. (15) must take a value greater than zero and the negative value in Eq. (16) for the constant *c* is not physically realistic. As the drop size tends to zero in Eq. (15) the stain size also tends to zero as would be expected.

Although it is not physically realistic (as when the velocity tends to zero the stain size tends to zero), to compare results to those in Refs. (17,18), the equation for the Reynold's number was forced to pass through zero giving *c* = 0 in Eq. (15) as in Eq. (6) taken from Ref. (17). This gave correlation coefficients of *R*<sup>2</sup> = 0.81 and 0.83 for *Re* and *Re*<sup>0.5</sup>, respectively, with equations  $\alpha = 0.00310 \text{ Re}$  or  $\alpha = 0.200 \text{ Re}^{0.5}$ . The original for *Re*<sup>0.5</sup> had a coefficient of 0.5 for water droplets (18), but it was found necessary to alter this to 0.555 for the work on blood (17). This compares with the equivalent coefficient here of 0.2<sup>2</sup> = 0.4, suggesting differences in the results.

Even better results are obtained with correlation coefficients of *R*<sup>2</sup> = 0.95 and 0.93 by plotting the stain size against *Re*<sub>IM</sub>*D*<sub>o</sub>*D*<sub>o</sub> and *ReD*<sub>o</sub>*D*<sub>o</sub>. Mathematically, these variables give equations of the form:

$$ab = m_1 M D_o^2 + c_1 \quad (17)$$

where *m*<sub>1</sub> and *c*<sub>1</sub> are constants and *M* is a nondimensional number such as the Reynolds number or *Re*<sub>IM</sub>. When the velocity tends to zero the stain size tends to the value of *c*<sub>1</sub>; however, *c*<sub>1</sub> is a constant and it would be expected that the stain size formed when a droplet is placed on the surface (with zero velocity) would vary with drop size. When the drop size tends to zero then again the stain size tends to the value of *c*<sub>1</sub>, when clearly it should tend to zero. When *c*<sub>1</sub> is zero then as the drop size tends to zero the stain size correctly tends to zero. However, as the velocity tends to zero the stain size also tends to zero when actually although it should become smaller it should tend towards a size based on the drop size.

For the number of spines, significant correlations were found (Table 2) for the Reynold's number, the square root of the Weber number, *Re*<sub>1</sub> and *Re*<sub>IM</sub>. Once the equations are forced to pass through zero, implying no spines when the velocity or drop size tend to zero, the correlation coefficient for the Weber number becomes insignificant but the other parameters still show significant correlations. Compared to the results from Ref. (5,17), where the number of spines from Eq. (7) was *C*<sub>n</sub> = 0.955 and 1.11, respectively, here the value for *C*<sub>n</sub> was 0.63.

**Angled Impact**

When all the angles (from 22.7° to 90° to the horizontal) are considered, the correlation coefficients on the right of Table 1 are obtained for the stain size. To calculate the stain size using alpha, the only significant correlation is against the Reynolds number (Fig. 4) when *R*<sup>2</sup> = 0.8. A significant correlation is also obtained for the square root of the Reynolds number, but as in the vertical impact case, the negative constant means that the stain's size tends to a negative area as the velocity tends to zero, nullifying this equation.

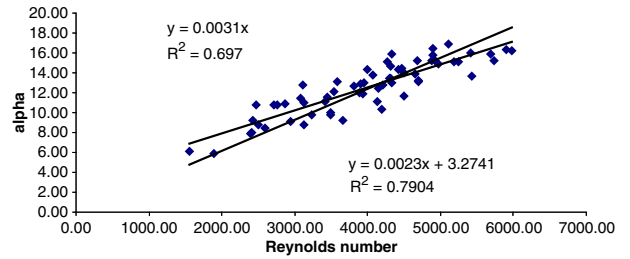


FIG. 4—Plot of alpha against Reynolds number.

As discussed in the section on vertical impact, an equation relating alpha to the impact velocity and drop size, when the line does not pass through zero gives the best physical interpretation of the data when the velocity or drop size tend to zero. However, better correlations were found for the stains size against *ReDD*, *Re*<sub>1</sub>*D*<sub>o</sub>*D*<sub>o</sub>, and *Re*<sub>IM</sub>*D*<sub>o</sub>*D*<sub>o</sub>. The best correlation was for *Re*<sub>IM</sub>*D*<sub>o</sub>*D*<sub>o</sub> (Fig. 5) with a correlation coefficient of *R*<sup>2</sup> = 0.88.

For the number of spines none of the parameters give a significant correlation (Table 2). However, the graphs do not take into account the angle of impact, which alters the stain's shape. To take this into consideration the graphs were replotted in the form:

$$y = m \times \sin^n \theta + c \quad (18)$$

where  $\theta$  is the impact angle and *n* is a constant, varied to give the best fit. Correlation coefficients are given in Table 3.

These results include the data collected at 22.7° to the horizontal. The number of spines tends toward a single spine as the impact velocity and impact angle tend to zero. This means that at low impact velocities and angles, it is impossible to distinguish between stains by calculating the number of spines. However, for the experiments carried out for the impact angle at 22.7° to the horizontal, it was found that whilst droplets from 50 cm only formed one spine (Fig. 6a) those at faster impacts (from 100 cm and above) formed more than one spine (Fig. 6b). This suggests that whilst the correlations are still valid at this angle, further work would be needed, for example, looking at spine length, to consider smaller angles and lower velocity impacts when only one spine is formed.

For the stain size the best results occur when the angle of impact is neglected, i.e., *n* = 0 in Eq. (18). This implies that the stain size is independent of the angle of impact. This is feasible in that regardless of the impact angle the same amount of blood is available and a change in stain size would only occur if significant cast off occurs or the blood collects at one end of a long stain or a stain is exceptionally thick. There was no clear sign of these occurring.

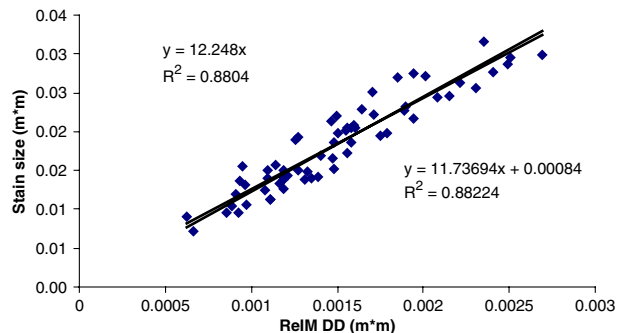


FIG. 5—Plot of stain size against *Re*<sub>IM</sub>*D*<sub>o</sub>*D*<sub>o</sub>.

TABLE 3—Correlation coefficients,  $R^2$ , for experimental results taking into account varying impact angle with, in brackets, the most significant equation for the number of spines.

Equation fitted	$n$							
	-2	-1	0	0.5	1	2	3	4
$\alpha = mRe \sin^n \theta + c$	—	0.13	0.79	—	0.71	0.53	—	—
$\alpha = mRe^{0.5} \sin^n \theta + c$	—	0.00	0.80	0.72	0.53	0.34	—	—
$S = mReD_oD_o \sin^n \theta + c$	0.14	0.72	0.86	—	0.69	0.53	—	—
$S = mReD_oD_o \sin^n \theta$	—	0.66	0.80	—	0.69	—	—	—
$S = mRe_{IM}D_oD_o \sin^n \theta + c$	—	0.63	0.88	—	0.65	—	—	—
$S = mRe_{IM}D_oD_o \sin^n \theta$	—	0.61	0.88	—	0.47	—	—	—
$N = mRe \sin^n \theta + c$	—	0.06	0.29	—	0.75	0.89	0.93 (y = 0.0068x + 1.60)	0.92
$N = mRe \sin^n \theta$	—	—	0.29	—	0.72	0.89	0.92 (y = 0.92x)	0.88
$N = mWe^{0.5} \sin^n \theta + c$	—	0.1	0.21	—	0.072	0.87	0.91 (y = 0.72x + 1.27)	0.9
$N = mWe^{0.5} \sin^n \theta$	—	—	0.21	—	0.68	0.86	0.90 (y = 0.76x)	0.87
$N = mRe_I D_o D_o \sin^n \theta + c$	—	—	0.26	—	0.74	0.89	0.92 (y = 0.070x + 1.39)	0.92
$N = mRe_I D_o D_o \sin^n \theta$	—	—	0.26	—	0.70	0.88	0.92 (y = 0.074x)	0.88
$N = mRe_{IM} D_o D_o \sin^n \theta + c$	—	—	0.24	—	0.71	0.89	0.93 (y = 0.34x - 0.02)	0.89
$N = mRe_{IM} D_o D_o \sin^n \theta$	—	—	0.25	—	0.81	0.92	0.93 (y = 0.32x)	0.92

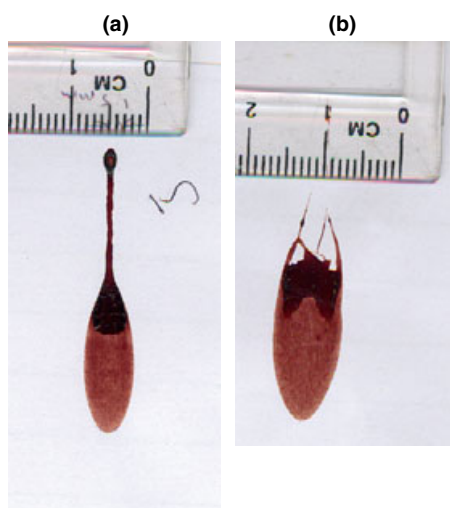


FIG. 6—Blood stains falling from a small sized pipette at an angle of 22.7° to the vertical from (a) 5 and (b) 200 cm.

As discussed above, physically, the best equation to use is that for the Reynolds number given by:

$$\alpha = 0.0023Re + 3.27 \tag{19}$$

as the equation makes physical sense as the velocity and drop size tend to zero. Better fits are found using  $ReD_oD_o$ ,  $Re_I D_oD_o$ , and  $Re_{IM} D_oD_o$  but they do not give the correct result as the velocity tends to zero. However, as long as the equation is only used within the limits of the collected data then the other equations could be used, for example, the equation for  $Re_{IM} D_oD_o$  with  $R^2 = 0.88$ , compares with  $R^2 = 0.70$  for Eq. (19) gives

$$ab = 111.74Re_{IM}D_oD_o + 0.00084 \tag{20}$$

For the number of spines, the angle of impact has a clear effect (see Fig. 1). Whilst there is no correlation when  $n$  is set to 0, for  $n = 3$  Reynolds number, Weber number,  $Re_I$  and  $Re_{IM}$  all give correlations of better than 0.9. Example plots, for  $Re$  and  $We^{0.5}$  are given in Figs. 7 and 8, respectively. For the Weber number this cubic dependence on the impact angle could be due to the variable parameter  $D_oV_o^2$ , but for  $We^{0.5}$ ,  $Re$ ,  $Re_I$ , and  $Re_{IM}$  the reason for this cubic dependency of the angle is unclear.

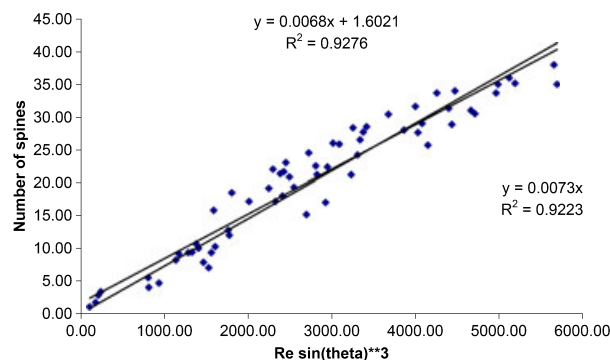


FIG. 7—Plot of the number of spines against  $Re \sin^3(\theta)$ .

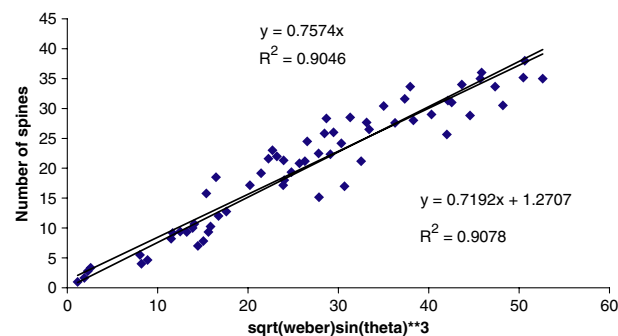


FIG. 8—Plot of the number of spines against  $We^{0.5} \sin^3(\theta)$ .

A summary on the causes of spines is given in Ref. (5), outlining that at the moment, it is thought that the number of spines depends on the surface tension of a liquid and not its viscosity. Given the closeness of the correlation coefficients, this means that from this data it is not possible to determine which equation is best. Until more data varying the density, surface tension, viscosity, and surface can be obtained it is recommended that the equation using the square root of the Weber number is used. Given that it would be expected that the number of spines should tend to zero as the drop size or velocity tend to zero then:



$$N = 0.76We^{0.5} \sin^3 \theta \quad (21)$$

The coefficient in Eq. (21) is 0.76, this is lower than those in Refs. (17) and (5), 0.955 and 1.11, respectively. The difference in values may be due to the difference in surface used. The surface affects the contact angle between the liquid and the surface and hence the stain size (18). Another possible explanation is that, as was observed in Ref. (17), counting spines is somewhat subjective. The author's experience with working with water and now blood has shown that it is more important to be consistent than to obtain the exact number of spines. As long as the counter is consistent then the same relationships will occur, with slightly different coefficients, hence until the process can be automated a researcher must obtain and apply their own equations to work in the field.

### Conclusions

The experimental work presented in this paper shows that it is possible to use a single equation to take into account the impact angle when calculating a blood stain's size and number of spines. Hence for a blood droplet's impact on paper by measuring the stains size and number of spines it is possible to determine the impact velocity and hence the position of the source of the droplet.

The results differ from those of Hulse-Smith et al. (17), but different surfaces were used and as they point out the determination of what is a spine is difficult to quantify. Results at Cranfield University have shown that as long as the person counting spines is always consistent meaningful equations can be found and used. The exact form of the equation to determine the number of spines will require further work using different liquids to determine the exact dependency of the number of spines.

Currently, work has only been carried out on paper and further work will be needed to determine whether any relationships exist for other surfaces and if they can also be incorporated into a single equation for all surfaces by taking account of the contact angle and/or the surface roughness. Before use at crime scenes the work will then have to be validated using blind trials. For crime scene work, it may also be possible to set up equations that do not need the liquid's density, viscosity, and surface tension, the values of which will have to be taken from the literature, as they cannot be obtained from a dried scene. However, this will make it more difficult to include effects such as different surfaces or extend the work to other liquids found at a crime scene and still have a single equation.

### References

1. MacDonell HL. *Bloodstain patterns*. Corning, NY: Laboratory of Forensic Science, 1993.
2. Bevel T, Gardner RM. Determining the point of convergence and the point of origin. In: Bevel T, Gardner RM, editors. *Bloodstain pattern analysis: with an introduction to crime scene reconstruction*. London: CRC Press Inc., 2002;121–41.
3. Young HD. *University physics*. Reading, MA: Addison-Wesley Publishing Company, 1992.
4. Asai A, Shioya M, Hirasawa S, Okazaki T. Impact of an ink drop on paper. *J Imaging Sci Technol* 1993;37(2):205–7.
5. Mehdizadeh NZ, Chandra S, Mostaghimi J. Formation of fingers around the edge of a drop hitting a metal plate. *J Fluid Mech* 2004;510:353–73.
6. Thoroddsen ST, Sakakibara J. Evolution of the fingering pattern of an impacting drop. *Phys Fluids* 1998;10(6):1359–74.
7. Chang W-J, Hills DJ. Sprinkler droplet effects on irrigation. I: impact simulation. *J Irrig Drain E-ASCE* 1993;119(1):142–56.
8. Ford RE, Furnidge CGL. Impact and spreading of spray drops on foliar surfaces. *Soc Chem Ind Monogr* 1967;25:417–32.
9. Cheng L. Dynamic spreading of drops impacting onto a solid surface. *Ind Eng Chem Process Des Dev* 1977;16(2):192–7.
10. Scheller BL, Bousfield DW. Newtonian drop impact with a solid surface. *AICHE J* 1995;41(6):1357–67.
11. Rein M. Phenomena of liquid drop impact on solid and liquid surfaces. *Fluid Dyn Res* 1993;12:61–93.
12. Mao T, Kuhn DCS, Tran H. Spread and rebound of liquid droplets upon impact on flat surfaces. *AICHE J* 1997;43(9):2169–79.
13. Allen RT. The role of surface tension in splashing. *J Colloid Interf Sci* 1974;51(2):350–1 (Letter to Editor).
14. Davidson MR. Boundary integral prediction of the spreading of an inviscid drop impacting on a solid surface. *Chem Eng Sci* 2000;55:1159–70.
15. Fukai J, Zhao Z, Poulidakos D, Megaridis CM, Miyatake O. Modeling of the deformation of a liquid droplet impinging on a flat surface. *Phys Fluids A* 1993;5(11):2588–99.
16. Marmanis H, Thoroddsen ST. Scaling of the fingering pattern of an impacting drop. *Phys Fluids* 1996;8(6):1344–6.
17. Hulse-Smith L, Mehdizadeh NZ, Chandra S. Deducing drop size and impact velocity from circular bloodstains. *J Forensic Sci* 2005;50:54–63.
18. Pasandideh-Fard M, Qiao YM, Chandra S, Mostaghimi SJ. Capillary effects during droplet impact on a solid surface. *Phys Fluids* 1996;8(3):650–9.
19. Kang BS, Lee DH. On the dynamic behavior of a liquid droplet impacting upon an inclined heated surface. *Exp Fluids* 2000;29:380–7.
20. Bussman M, Mostaghimi J, Chandra S. On the three dimensional volume tracking model of droplet impact. *Phys Fluids* 1999;11(6):1406–17.
21. Raymond MA, Smith ER, Leisegang J. The physical properties of blood – forensic considerations. *Sci Justice* 1995;36:153–60.

Additional information and reprint requests:

Clare Knock, M.D.  
Engineering Systems Department  
Cranfield University  
Shrivenham, Swindon  
Wilts SN6 8BB, U.K.  
E-mail: c.knock@cranfield.ac.uk